Inorganic Chemistry
Communication
Cite This: Inorg. Chem. 2020, 59, 193−197
pubs.acs.org/IC

Magnetooptical Properties of Chiral [Co_2Ln] Clusters

Yu-Jia Zhang, Gang Wu, Han Xu, Xing Wang, La-Sheng Long, Xiang-Jian Kong,* and Lan-Sun Zheng

Collaborative Innovation Center of Chemistry for Energy Materials, State Key Laboratory of Physical Chemistry of Solid Surfaces, and Department of Chemistry, College of Chemistry and Chemical Engineering, Xiamen University, Xiamen 361005, China

Supporting Information

ABSTRACT: Two pairs of enantiomeric 3d−4f metal clusters, [$Co_2Ln[(R)/(S)\text{-L}]_4]\cdot Cl_5\cdot(H_2O)_2\cdot CH_3OH\cdot CH_3CH_2OH$ [**Co_2Ln**; Ln = Gd (**1S** and **1R**), Dy (**2S** and **2R**)], were synthesized by the reaction of chiral Schiff-base ligand (*R*)/(*S*)-3-[(2-hydroxybenzylidene)amino]propane-1,2-diol [(*R*)/(*S*)-HL] with $CoCl_2\cdot 6H_2O$ and $LnCl_3\cdot 6H_2O$. The circular dichroism spectra of (***S***)/(***R***)-**Co_2Ln** display a mirror-symmetry effect with seven peaks at 210−800 nm, which can be ascribed to $\pi-\pi^*$ transitions, exciton coupling, charge-transfer transitions between ligands and Co^{3+}, and characteristic d−d transitions of Co^{3+} ions. Interestingly, the chiral **Co_2Ln** metal clusters display strong magnetic circular dichroism signals at room temperature. This work suggests that the chiromagnetic metal cluster is expected to show a strong magnetooptical response.

The magnetooptical Faraday effect has attracted much attention because of its important application in magnetooptical devices such as magnetooptical isolators, magnetooptical switches, fiber-optic magnetooptical sensors, and optical current transformers.[1] As a manifestation of the Faraday effect, magnetic circular dichroism (MCD) has become the predominant technique to investigate electronic transitions in magnetooptical materials because, arising from the magnetic-field-induced Zeeman interactions, the MCD response is a universal property of all matter. So, the study of MCD mainly focuses on achiral substances. The introduction of chirality into the magnetooptical materials can produce very interesting magnetooptical phenomena, such as magnetochiral dichroism (MChD), which displays a junction of the chirality and magnetism.[2] However, up to now, only a few of the chiral systems, such as chiral nanoparticles,[2a,3] organic aromatic π-conjugated systems,[2c−e] and coordination compounds,[2g,i,4] had been explored to study the MCD and MChD properties. A recent study showing that the chiral medium itself has magnetic centers is a crucial factor expected to obtain the large magnetochiral response.[2f] Therefore, chiromagnetic materials, with molecular magnetism, will be ideal systems for obtaining a large magnetooptical effect. However, there are few investigations about the Faraday effect in chiromagnetic materials.

Chiral lanthanide−transition metal (3d−4f) clusters are ideal molecular magnets for studying the magnetooptical response.[2f,5] Compared with other chiral materials,[6] chiral 3d−4f metal clusters not only have rigid chiral structures but also have multiple magnetic centers (3d and 4f metal ions), which is favorable for obtaining larger chiroptical properties and the Faraday effect.[5,7] At the same time, the rich and adjustable magnetic interactions between multiple metal ions provides an ideal platform for studying the magnetooptical effect. Following this idea, here we prepared a pair of chiral Schiff-base ligands (*R*)/(*S*)-3-[(2-hydroxybenzylidene)amino]-propane-1,2-diol [(*R*)/(*S*)-HL] and synthesized two pairs of chiral 3d−4f clusters with formulas of [$Co_2Ln[(R)/(S)\text{-L}]_4]\cdot Cl_5\cdot(H_2O)_2\cdot CH_3OH\cdot CH_3CH_2OH$ (namely, **Co_2Ln**; Ln = Gd for **1S** and **1R** and Dy for **2S** and **2R**). The Faraday effect of the chiral 3d−4f clusters is also investigated using MCD.

The clusters **Co_2Ln** were obtained by reaction with the chiral Schiff-base ligand (*R*)/(*S*)-HL, Ln^{3+}, Co^{2+}, and triethylamine in a mixed methanol/ethanol solvent. Single-crystal X-ray diffraction results confirmed that compounds **1S**/**1R** and **2S**/**2R** crystallized in the chiral $P2_12_12$ space group. The structures of complexes **1S**/**1R** and **2S**/**2R** are isostructural, so only **1S** was selected as the representative to describe the crystal structure in detail. As shown in Figure 1, the crystal structure of the cluster **1S** looks like a butterfly, the wings are formed by the coordination of two Schiff-base ligands and Co^{III} ions, and the body is a Gd^{III} ion. Compound **1S** consists of one cationic cluster of $[Co_2Gd(C_{10}H_{12}NO_3)_4]^{5+}$, $5Cl^-$, and guest molecules. In the cation cluster, there are three metal ions where the Gd^{III} ion is the center and the two Co^{III} ions are on

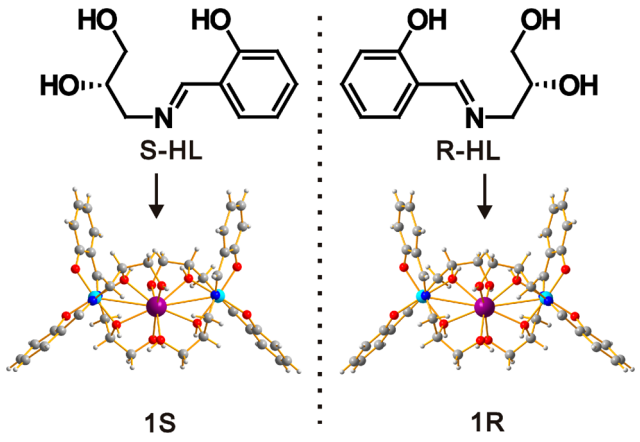

Figure 1. Chemical structures of the (*R*)/(*S*)-HL ligands and crystal structures of **1S** and **1R**. Color code: Ln, purple; Co, blue; O, red; C, gray; H, white.

Received: October 23, 2019
Published: December 20, 2019

DOI: 10.1021/acs.inorgchem.9b03115
Inorg. Chem. 2020, 59, 193−197

both sides. The adjacent two Co^{III} ions and one Gd^{III} ion were bridged by four μ_2-propanediol O atoms, forming a linear trinuclear structure. The distances between the central Gd^{III} ion and two terminal Co^{III} ions are 3.415(10) and 3.426(11) Å, respectively. The central Gd^{III} ion adopts a distorted square-antiprismatic coordination geometry (Figure S1b), coordinated by eight O atoms of propanediol from four (*S*)-L^- ligands. Each Co^{III} ion adopts the same coordination mode, which is six-coordinated with a distorted octahedral coordination geometry (Figure S1a), ligated by two N atoms of the methylamine, two phenol hydroxyl O atoms, and two O atoms of propanediol from two (*S*)-L^- ligands. The Co1−O/N and Co2−O/N bond distances and Gd−O bond distances are in the ranges of 1.874(12)−1.921(12) and 2.341(9)−2.441(9) Å, respectively; both are similar to those reported for other Co_2Ln complexes in the literature.[8]

In order to investigate the optical activity and magneto-optical properties, UV−visible absorption, liquid circular dichroism (CD), and MCD in an EtOH solvent (0.5 and 0.05 g·L^{-1}) were measured. As shown in Figure 2a, the UV−visible spectra of compounds **1S**, **1R**, **2S**, and **2R** exhibit nearly identical peaks in the range of 210−800 nm, with strong peaks at 252 and 379 nm, a shoulder at 317 nm, and weak peaks at about 535 and 697 nm. The peak at 252 nm in the UV region was assigned to $\pi-\pi^*$ transitions of the aromatic groups of the ligands, the peak at 379 nm was attributed to the $\pi-\pi^*$ conjugate interactions between aromatic rings and an azomethine chromophore, and the broad shoulder at 317 nm was attributed to $\pi-\pi^*$ transitions of an azomethine chromophore. The weak absorption at 535 nm was attributed to charge-transfer transitions between the Co^{III} ions and ligands, and the lowest intense peak around 700 nm corresponded to d−d transitions of the Co^{III} ions.

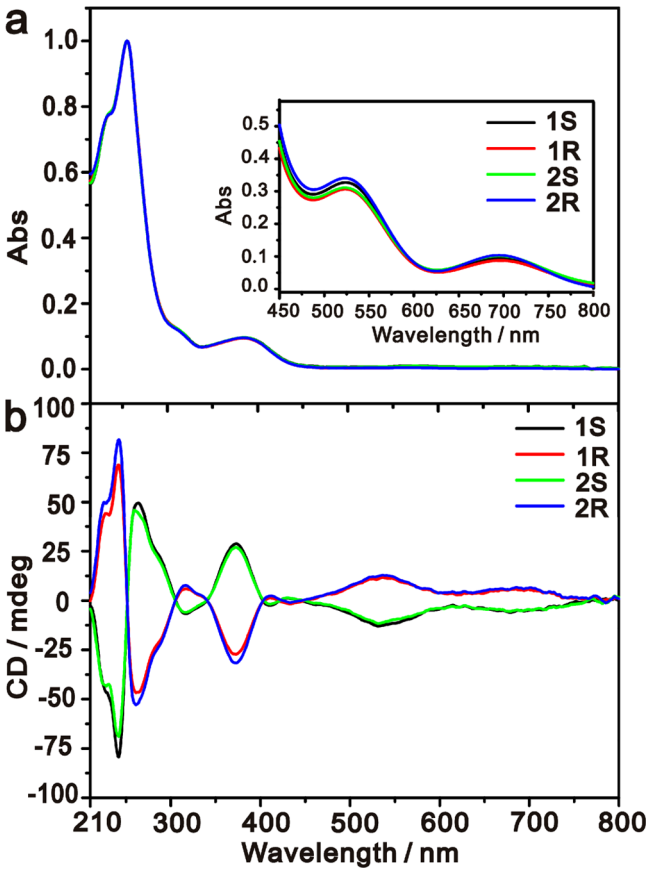

Figure 2. (a) UV−visible spectrum (c = 0.05 g·L^{-1}) of **1S**, **1R**, **2S**, and **2R** in an EtOH solution. The inset shows the UV−visible spectrum at high concentration (c = 0.5 g·L^{-1}). (b) CD spectra (c = 0.05 g·L^{-1}) of **1S**, **1R**, **2S**, and **2R** in an EtOH solution.

The CD spectra of the enantiomeric compounds **1S**, **1R**, **2S**, and **2R** are nearly perfect mirror images with up to seven peaks in the range of 800−210 nm. As shown in Figure 2b, the spectral positions of the CD peaks are roughly aligned with those in the UV−visible spectra, which correspond to various transitions. The CD spectra exhibit two split peaks around 242 and 261 nm, which can be ascribed to excitonic coupling for $\pi-\pi^*$ transitions of the aromatic groups, the peak at 317 nm was attributed to $\pi-\pi^*$ transitions of azomethine chromophores, and the CD split peak at 400 nm is derived from exciton coupling, which was caused by aggregation of the chromophores.[9] Compared with the UV−visible spectral peak at 379 nm, the CD peak at 400 nm is red-shifted, which may be caused by a conjugated effect between the ligands in the cluster. The intense CD signals of these chiral 3d−4f clusters in the range of 210−450 nm were obtained by the exciton chirality of the twisted configuration between aromatic rings and azomethine chromophores.[10] Also, the other two peaks in the range of 500−800 nm correspond to charge-transfer transitions between the ligands and Co^{III} ions and d−d transitions of Co^{III} ions. Compounds **2S** and **2R** show CD peaks very similar to those of **1S** and **1R**. Compared with the CD spectrum of the ligands (Figure S6a), the rigid structure of the chiral 3d−4f metal clusters has enhanced chirality signals.

To study the magnetooptical properties, CD under an external magnetic field (1.6 T) at room temperature was performed. For the convenience of description, we specify that the positive direction (+1.6 T, N−S) of the magnetic field is parallel to the polarized light and the opposite direction (−1.6 T, S−N) is antiparallel to the polarized light. As shown in Figure 3, the CD signal intensities of **1S**/**1R** under +1.6 and −1.6 T around 252, 317, 400, and 535 nm are significantly different from the CD signals without a magnetic field (0 T). As shown in Figure 3b, the positive-direction magnetic field (+1.6 T) has a negative effect on the CD signals of the split peak at 252 nm for the two configurations, while the negative-direction magnetic field (−1.6 T) has a positive effect. As shown in Figure 3c−f, the effects of the magnetic field on the split peak at 400 nm and the peak at 535 nm have trends similar to that of 252 nm, but the effect on the signal at 317 nm is reversed. The effect of the magnetic field on the CD intensity of **2R** and **2S** is the same as that of **1S** and **1R** (Figure S7). These results show that the effect of the magnetic field with orientations parallel and antiparallel to the light propagation direction on the CD signals is completely opposite.

In order to study the magnetooptical properties more clearly, the pure MCD signals were calculated with the formulas CD(+1.6 T) = CD(0 T) + MCD (**1**), CD(−1.6 T) = CD(0 T) − MCD (**2**), and MCD = [CD(+1.6 T) − CD(−1.6 T)]/2 (**3**). The pure MCD signs of **1S** to **2R** are shown in Figure 4. The obvious Faraday effect of the positive magnetic field on the CD signal intensity was opposite to that of the antimagnetic field for compounds of the same configuration. When the magnetic field is applied in the same direction, the effect of the magnetic field on the CD signal intensity of the enantiomer is the same. We can see that the strong MCD

DOI: 10.1021/acs.inorgchem.9b03115
Inorg. Chem. 2020, 59, 193−197

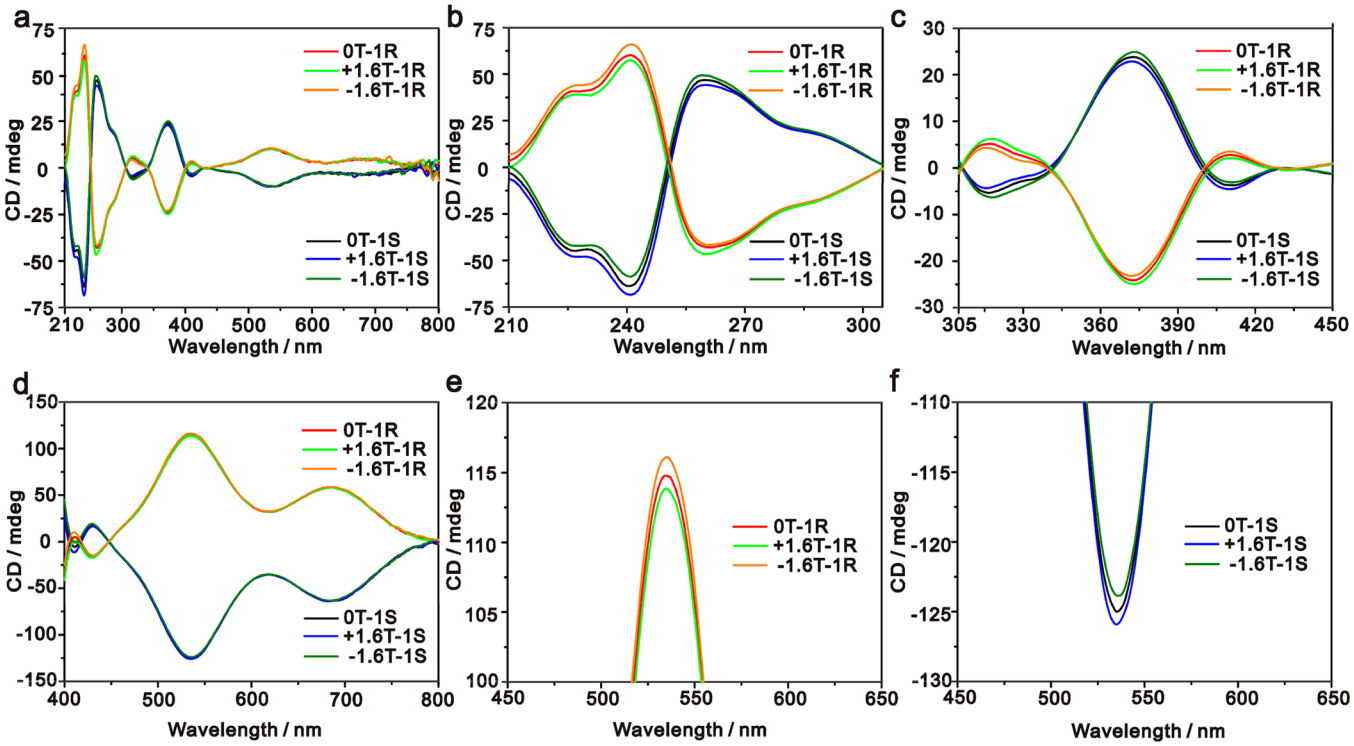

Figure 3. CD spectra of **1S** and **1R** in an EtOH solution (c = 0.05 g·L^{-1}; H = 0 and 1.6 T) in the ranges of (a) 210−800, (b) 210−305, and (c) 305−450 nm. CD spectra of **1S** and **1R** in an EtOH solution (c = 0.5 g·L^{-1}; H = 0 and 1.6 T) in the range of (d) 400−800 nm. CD spectra of (e) **1R** and (f) **1S** in an EtOH solution (c = 0.5 g·L^{-1}; H = 0 and 1.6 T) in the range of 450−650 nm.

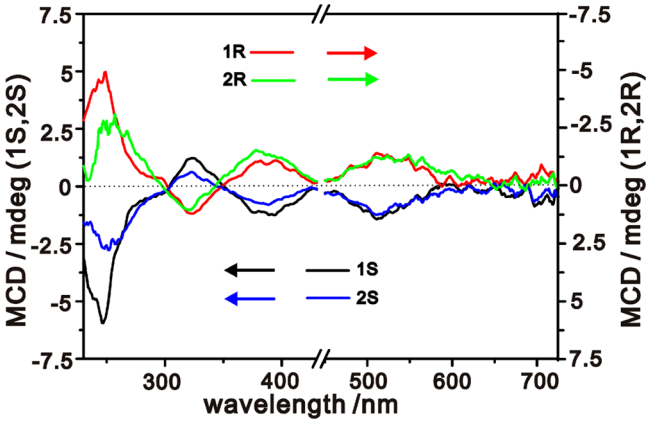

Figure 4. MCD spectra of **1S**, **2S**, **1R**, and **2R** in an EtOH solution (H = 1.6 T) in the ranges of 230−450 nm (0.05 g·L^{-1}) and 450−720 nm (0.5 g·L^{-1}).

signals in the range of 210−450 nm were attributed to the large orbital angular momentum of aromatic π-conjugated systems, which were similar to the MCD signals of organic compounds.[11] In the range of 450−725 nm, a weak MCD signal around 535 nm is observed, and the MCD signal originating from the d−d transition of octahedral Co^{III} ions in the range of 650−725 nm is weaker than those of other signals.[12] Compared with the MCD spectrum of the ligand (Figure S6b), the rigid structure of the chiral 3d−4f metal clusters produces more and stronger MCD signals, indicating that the 3d−4f metal clusters have a larger Faraday effect. Notably, the value of g_{max}(MCD) is about 0.07 T^{-1}, which is comparable to strong g_{MCD} values for molecular complexes in the literature.[4d] Meanwhile, the corresponding maximum value of g_{max}(CD) is 0.20. So, the magnitude of g_{MChD} can be roughly estimated with a large value of 7×10^{-3} T^{-1} by the formula $g_{MChD} = g(CD)\, g(MCD)/2$.[2a,b] The result indicates that chiral 3d−4f clusters are likely to produce the large g_{MChD} values.[2a−d,h]

In summary, two pairs of enantiomeric 3d−4f metal clusters were synthesized based on the chiral Schiff-base ligands. Chiral Schiff-base ligands and 3d−4f metal ions are assembled into clusters with rigid structures, not only generating a distorted configuration between the aromatic rings and azomethine chromophores, which generates strong exciton chirality, but also inducing chirality to the 3d metal center. The influence of a static magnetic field with orientations parallel and antiparallel to the light propagation direction on the CD signals is completely opposite. This work suggested that strong MChD possessing strong CD and MCD effects may be obtained in chiromagnetic metal clusters by combining chirality and magnetism. This work provides a reference for the design of magnetooptical materials with a strong MChD effect.

■ ASSOCIATED CONTENT

Supporting Information

The Supporting Information is available free of charge at https://pubs.acs.org/doi/10.1021/acs.inorgchem.9b03115.

Experimental section, Tables S1−S5, and additional Figures S1−S7 of the structures (PDF)

Accession Codes

CCDC 1961042−1961045 contain the supplementary crystallographic data for this paper. These data can be obtained free of charge via www.ccdc.cam.ac.uk/data_request/cif, or by emailing data_request@ccdc.cam.ac.uk, or by contacting The

DOI: 10.1021/acs.inorgchem.9b03115
Inorg. Chem. 2020, 59, 193−197

Cambridge Crystallographic Data Centre, 12 Union Road, Cambridge CB2 1EZ, UK; fax: +44 1223 336033.

■ AUTHOR INFORMATION

Corresponding Author

*Email: xjkong@xmu.edu.cn (X.-J.K).

ORCID

La-Sheng Long: 0000-0002-0398-4709

Xiang-Jian Kong: 0000-0003-0676-6923

Notes

The authors declare no competing financial interest.

■ ACKNOWLEDGMENTS

This work was supported by the National Natural Science Foundation of China (Grants 21871224, 21673184, 21431005, and 21721001) and the Fundamental Research Funds for the Central Universities (Grant 20720180032).

■ REFERENCES

(1) (a) Bahuguna, R.; Mina, M.; Tioh, J. W.; Weber, R. J. Magneto-Optic-Based Fiber Switch for Optical Communications. *IEEE Trans. Magn.* **2006**, *42*, 3099−3101. (b) Bentley, A. K.; Ellis, A. B.; Lisensky, G. C.; Crone, W. C. Suspensions of nickel nanowires as magneto-optical switches. *Nanotechnology* **2005**, *16*, 2193−2196. (c) Kang, M. S.; Butsch, A.; Russell, P. S. J. Reconfigurable light-driven opto-acoustic isolators in photonic crystal fibre. *Nat. Photonics* **2011**, *5*, 549−553. (d) Liu, H.; Zhan, G.; Wu, G.; Song, C.; Wu, X.; Xu, Q.; Chen, X.; Hu, X.; Zhuang, N.; Chen, J. Improved Edge-Defined Film-Fed Growth of Incongruent-Melting $Tb_3Al_5O_{12}$ Crystal with High Magneto-Optical and Thermal Performances. *Cryst. Growth Des.* **2019**, *19*, 1525−1531. (e) Lu, H.; Wang, X.; Zhang, S.; Wang, F.; Liu, Y. A fiber-optic sensor based on no-core fiber and Faraday rotator mirror structure. *Opt. Laser Technol.* **2018**, *101*, 507−514. (f) Roubeau, O.; Colin, A.; Schmitt, V.; Clerac, R. Thermoreversible gels as magneto-optical switches. *Angew. Chem., Int. Ed.* **2004**, *43*, 3283−3286. (g) Snetkov, I. L.; Yakovlev, A. I.; Permin, D. A.; Balabanov, S. S.; Palashov, O. V. Magneto-optical Faraday effect in dysprosium oxide (Dy_2O_3) based ceramics obtained by vacuum sintering. *Opt. Lett.* **2018**, *43*, 4041−4044. (h) Sun, L.; Jiang, S.; Marciante, J. R. All-fiber optical magnetic-field sensor based on Faraday rotation in highly terbium-doped fiber. *Opt. Express* **2010**, *18*, 5407−5412. (i) Varvaro, G.; Di Trolio, A.; Polimeni, A.; Gabbani, A.; Pineider, F.; de-Julián-Fernández, C.; Barucca, G.; Mengucci, P.; Amore Bonapasta, A.; Testa, A. M. Giant magneto-optical response in H^+ irradiated $Zn_{1-x}Co_xO$ thin films. *J. Mater. Chem. C* **2019**, *7*, 78−85.

(2) (a) Eslami, S.; Gibbs, J. G.; Rechkemmer, Y.; van Slageren, J.; Alarcón-Correa, M.; Lee, T. C.; Mark, A. G.; Rikken, G. L. J. A.; Fischer, P. Chiral Nanomagnets. *ACS Photonics* **2014**, *1*, 1231−1236. (b) Rikken, G. L. J. A.; Raupach, E. Observation of magneto-chiral dichroism. *Nature* **1997**, *390*, 493−494. (c) Kitagawa, Y.; Miyatake, T.; Ishii, K. Magneto-chiral dichroism of artificial light-harvesting antenna. *Chem. Commun.* **2012**, *48*, 5091−5093. (d) Kitagawa, Y.; Segawa, H.; Ishii, K. Magneto-chiral dichroism of organic compounds. *Angew. Chem., Int. Ed.* **2011**, *50*, 9133−9136. (e) Ribo, J. M. Magnetochiral effects in amphiphilic porphyrin J-aggregates. *Angew. Chem., Int. Ed.* **2011**, *50*, 12402−12404. (f) Ceolin, M.; Goberna-Ferron, S.; Galan-Mascaros, J. R. Strong hard X-ray magnetochiral dichroism in paramagnetic enantiopure molecules. *Adv. Mater.* **2012**, *24*, 3120−3123. (g) Sessoli, R.; Boulon, M. E.; Caneschi, A.; Mannini, M.; Poggini, L.; Wilhelm, F.; Rogalev, A. Strong magneto-chiral dichroism in a paramagnetic molecular helix observed by hard X-ray. *Nat. Phys.* **2015**, *11*, 69−74. (h) Train, C.; Gheorghe, R.; Krstic, V.; Chamoreau, L. M.; Ovanesyan, N. S.; Rikken, G. L.; Gruselle, M.; Verdaguer, M. Strong magneto-chiral dichroism in enantiopure chiral ferromagnets. *Nat. Mater.* **2008**, *7*, 729−734. (i) Wang, K.; Zeng, S.; Wang, H.; Dou, J.; Jiang, J. Magneto-chiral dichroism in chiral mixed (phthalocyaninato)(porphyrinato) rare earth triple-decker SMMs. *Inorg. Chem. Front.* **2014**, *1*, 167−171.

(3) (a) Ceunen, W.; Van-Oosten, A.; Vleugels, R.; De-Winter, J.; Gerbaux, P.; Li, Z.; De-Feyter, S.; Verbiest, T.; Koeckelberghs, G. Synthesis and supramolecular organization of chiral poly(thiophene)-magnetite hybrid nanoparticles. *Polym. Chem.* **2018**, *9*, 3029−3036. (b) Smirnov, D. S.; Glazov, M. M. Stochastic Faraday rotation induced by the electric current fluctuations in nanosystems. *Phys. Rev. B: Condens. Matter Mater. Phys.* **2017**, *95*, 045406. (c) Woo, J. H.; Kang, B.; Gwon, M.; Lee, J. H.; Kim, D.-W.; Jo, W.; Kim, D. H.; Wu, J. W. Time-Resolved Pump-Probe Measurement of Optical Rotatory Dispersion in Chiral Metamaterial. *Adv. Opt. Mater.* **2017**, *5*, 1700141. (d) Yannopapas, V. Magnetochirality in hierarchical magneto-plasmonic clusters. *Solid State Commun.* **2015**, *217*, 47−52. (e) Yannopapas, V.; Vanakaras, A. G. Strong Magnetochiral Dichroism in Suspensions of Magnetoplasmonic Nanohelices. *ACS Photonics* **2015**, *2*, 1030−1038. (f) Yeom, J.; Santos, U. S.; Chekini, M.; Cha, M.; De-Moura, A. F.; Kotov, N. A. Chiromagnetic nanoparticles and gels. *Science* **2018**, *359*, 309−314.

(4) (a) Siddons, D. P.; Hart, M.; Amemiya, Y.; Hastings, J. B. X-ray optical activity and the Faraday effect in cobalt and its compounds. *Phys. Rev. Lett.* **1990**, *64*, 1967−1970. (b) Hasegawa, Y.; Maeda, M.; Nakanishi, T.; Doi, Y.; Hinatsu, Y.; Fujita, K.; Tanaka, K.; Koizumi, H.; Fushimi, K. Effective optical Faraday rotations of semiconductor EuS nanocrystals with paramagnetic transition-metal ions. *J. Am. Chem. Soc.* **2013**, *135*, 2659−2666. (c) Inoue, K.; Kikuchi, K.; Ohba, M.; Okawa, H. Structure and magnetic properties of a chiral two-dimensional ferrimagnet with TC of 38 K. *Angew. Chem., Int. Ed.* **2003**, *42*, 4810−4813. (d) Kitagawa, Y.; Wada, S.; Yanagisawa, K.; Nakanishi, T.; Fushimi, K.; Hasegawa, Y. Molecular Design Guidelines for Large Magnetic Circular Dichroism Intensities in Lanthanide Complexes. *ChemPhysChem* **2016**, *17*, 845−849. (e) Nakanishi, T.; Suzuki, Y.; Doi, Y.; Seki, T.; Koizumi, H.; Fushimi, K.; Fujita, K.; Hinatsu, Y.; Ito, H.; Tanaka, K.; Hasegawa, Y. Enhancement of optical Faraday effect of nonanuclear Tb (III) complexes. *Inorg. Chem.* **2014**, *53*, 7635−7641.

(5) Xing, Y.; Chen, L.-Q.; Zhao, Y.-R.; Zheng, X.-Y.; Zhang, Y.-J.; Kong, X.-J.; Long, L.-S.; Zheng, L.-S. High-Nuclearity Chiral 3d-4f Heterometallic Clusters Ln_6Cu_{24} and Ln_6Cu_{12}. *Inorg. Chem.* **2019**, *58*, 8494−8499.

(6) (a) Han, Z.; Shi, W.; Cheng, P. Synthetic strategies for chiral metal-organic frameworks. *Chin. Chem. Lett.* **2018**, *29*, 819−822. (b) Zhang, S.-Y.; Li, D.; Guo, D.; Zhang, H.; Shi, W.; Cheng, P.; Wojtas, L.; Zaworotko, M. J. Synthesis of a Chiral Crystal Form of MOF-5, CMOF-5, by Chiral Induction. *J. Am. Chem. Soc.* **2015**, *137*, 15406−15409. (c) Zhang, S.-Y.; Yang, C.-X.; Shi, W.; Yan, X.-P.; Cheng, P.; Wojtas, L.; Zaworotko, M. J. A Chiral Metal-Organic Material that Enables Enantiomeric Identification and Purification. *Chem.* **2017**, *3*, 281−289.

(7) Hu, P.; Wang, X.-N.; Jiang, C.-G.; Yu, F.; Li, B.; Zhuang, G.-L.; Zhang, T. Nanosized Chiral $[Mn_6Ln_2]$ Clusters Modeled by Enantiomeric Schiff Base Derivatives: Synthesis, Crystal Structures, and Magnetic Properties. *Inorg. Chem.* **2018**, *57*, 8639−8645.

(8) (a) Chandrasekhar, V.; Das, S.; Dey, A.; Hossain, S.; Kundu, S.; Colacio, E. Linear, Edge-Sharing Heterometallic Trinuclear $[Co^{II}$-Ln^{III}-$Co^{II}]$ (Ln^{III}=Gd^{III}, Dy^{III}, Tb^{III}, and Ho^{III}) Complexes: Slow Relaxation of Magnetization in the Dy^{III} Derivative. *Eur. J. Inorg. Chem.* **2014**, *2014*, 397−406. (b) Modak, R.; Sikdar, Y.; Thuijs, A. E.; Christou, G.; Goswami, S. Co^{II}_4, Co^{II}_7, and a Series of $Co^{II}_2Ln^{III}$ (Ln^{III}=Nd^{III}, Sm^{III}, Gd^{III}, Tb^{III}, Dy^{III}) Coordination Clusters: Search for Single Molecule Magnets. *Inorg. Chem.* **2016**, *55*, 10192−10202.

(9) (a) Ziegler, M. Charge-transfer excited state properties of chiral transition metal coordination compounds studied by chiroptical spectroscopy. *Coord. Chem. Rev.* **1998**, *177*, 257−300. (b) Cai, G.; Bozhkova, N.; Odingo, J.; Berova, N.; Nakanishi, K. Circular dichroism exciton chirality method. New red-shifted chromophores for hydroxyl groups. *J. Am. Chem. Soc.* **1993**, *115*, 7192−7198. (c) Gargiulo, D.; Ikemoto, N.; Odingo, J.; Bozhkova, N.; Iwashita, T.; Berova, N.; Nakanishi, K. CD Exciton Chirality Method: Schiff Base

DOI: 10.1021/acs.inorgchem.9b03115
Inorg. Chem. 2020, 59, 193−197

and Cyanine Dye-Type Chromophores for Primary Amino Groups. *J. Am. Chem. Soc.* **1994**, *116*, 3760−3767. (d) Matile, S.; Berova, N.; Nakanishi, K.; Novkova, S.; Philipova, I.; Blagoev, B. Porphyrins: Powerful Chromophores for Structural Studies by Exciton-Coupled Circular Dichroism. *J. Am. Chem. Soc.* **1995**, *117*, 7021−7022. (e) Seo, M. S.; Sun, D.; Kim, H. Stereoselective Chiral Recognition of Amino Alcohols with 2,2′-Dihydroxybenzil. *J. Org. Chem.* **2017**, *82*, 6586−6591.

(10) Hattori, S.; Ishii, K. Magneto-chiral dichroism of aromatic π-conjugated systems. *Opt. Mater. Express* **2014**, *4*, 2423−2432.

(11) Mack, J.; Stillman, M. J.; Kobayashi, N. Application of MCD spectroscopy to porphyrinoids. *Coord. Chem. Rev.* **2007**, *251*, 429−453.

(12) McCaffery, A. J.; Stephens, P. J.; Schatz, P. N. Magnetic optical activity of d-d transitions. Octahedral chromium (III), cobalt (III), cobalt (II), nickel (II), and manganese (II) complexes. *Inorg. Chem.* **1967**, *6*, 1614−1625.

DOI: 10.1021/acs.inorgchem.9b03115
Inorg. Chem. 2020, 59, 193−197